

Dalton Transactions

An international journal of inorganic chemistry

Accepted Manuscript

This article can be cited before page numbers have been issued, to do this please use: T. Xing, T. J. Prior, K. Chen and C. Redshaw, *Dalton Trans.*, 2021, DOI: 10.1039/D1DT00189B.



This is an Accepted Manuscript, which has been through the Royal Society of Chemistry peer review process and has been accepted for publication.

Accepted Manuscripts are published online shortly after acceptance, before technical editing, formatting and proof reading. Using this free service, authors can make their results available to the community, in citable form, before we publish the edited article. We will replace this Accepted Manuscript with the edited and formatted Advance Article as soon as it is available.

You can find more information about Accepted Manuscripts in the [Information for Authors](#).

Please note that technical editing may introduce minor changes to the text and/or graphics, which may alter content. The journal's standard [Terms & Conditions](#) and the [Ethical guidelines](#) still apply. In no event shall the Royal Society of Chemistry be held responsible for any errors or omissions in this Accepted Manuscript or any consequences arising from the use of any information it contains.

ARTICLE

Titanium complexes bearing oxa- and azacalix[4, 6]arenes: structural studies and use in the ring opening homo-/co-polymerization of cyclic esters

Tian Xing,^a Timothy J. Prior,^a Kai Chen^b and Carl Redshaw^{a*}Received 00th January 20xx,
Accepted 00th January 20xx

DOI: 10.1039/x0xx00000x

Abstract: Reaction of excess $[\text{Ti}(\text{O}i\text{Pr})_4]$ with *p*-tert-butyltetrahomodioxacalix[6]arene H_6 (L^1H_6) afforded, after work-up (MeCN), the complex $[\text{Ti}_2(\text{O}i\text{Pr})_2(\text{MeCN})\text{L}^1]\cdot 3.5\text{MeCN}$ (**1**·3.5MeCN), whilst the oxo complex $[\text{Ti}_4(\mu_3\text{-O})_2(\text{H}_2\text{O})(\text{L}^1)_2]\cdot \text{MeCN}$ (**2**·MeCN) was isolated via a fortuitous synthesis involving the use of two equivalents of $[\text{Ti}(\text{O}i\text{Pr})_4]$. Reactions of *p*-methyl-dimethyldiazacalix[6]arene H_6 (L^2H_6) with $[\text{TiF}_4]$ (four equivalents), $[\text{TiCl}_4(\text{THF})_2]$ (two equivalents) or $[\text{TiBr}_4]$ (>four equivalents) resulted in the titanium-based azacalix[*n*]arene complexes $[\text{Ti}_4\text{F}_{14}\text{L}^2\text{H}_2(\text{H})_2]\cdot 2.5\text{MeCN}$ (**3**·2.5MeCN), $[\text{Ti}_2\text{X}_4(\text{H}_2\text{O})_2\text{OL}^2\text{H}_2(\text{H})_2]$ (X = Cl (**4**·5MeCN), Br (**5**·4.5MeCN) and $[\text{Ti}_4\text{Br}_{12}\text{L}^2(\text{H})_2(\text{MeCN})_6]\cdot 7\text{MeCN}$ (**6**·7MeCN), respectively. Reaction of four equivalents of $[\text{TiF}_4]$ with L^3H_4 ($\text{L}^3\text{H}_4 = p$ -methyl-dimethyldiazacalix[4]arene H_4) afforded the product $[\text{Ti}_2\text{F}_2(\mu\text{-F})_3\text{L}^3(\text{H})_2(\text{SiF}_5)]\cdot 2\text{MeCN}$ (**7**·2MeCN). These complexes have been screened for their potential to act as pre-catalysts in the ring opening polymerization (ROP) of ϵ -caprolactone (ϵ -CL), δ -valerolactone (δ -VL) and *rac*-lactide (*r*-LA). Generally, the titanium complexes bearing oxacalixarene exhibited better activities than the azacalixarene-based pre-catalysts. For ϵ -CL, δ -VL and *r*-LA, moderate activity at 130 °C over 24 h was observed for **1**–**6**. In the case of the co-polymerization of ϵ -CL with *r*-LA, **1**–**6** afforded reasonable conversions and high molecular weight polymers; **7** exhibited lower catalytic performance due to low solubility. None of the complexes proved to be active in the polymerization of ω -pentadecalactone (ω -PDL) under the conditions employed herein.

Introduction

Calix[*n*]arenes are a family of macrocyclic molecules consisting of phenol units linked most commonly by methylene ($-\text{CH}_2-$) bridges at their *ortho* positions, and have found widespread use in supramolecular chemistry.^[1] Investigations into their coordination chemistry have shown that their potential in areas such as catalysis can be greatly improved if the methylene bridges are replaced by heteroatom-containing bridges such as thia ($-\text{S}-$), sulfinyl ($-\text{SO}-$), sulfonyl ($-\text{SO}_2-$) or dimethyleneoxa ($-\text{CH}_2\text{OCH}_2-$), which can potentially bind to the metal.^[2] Interestingly, there is a lack of such studies involving dimethyleneoxa ($-\text{CH}_2\text{OCH}_2-$) containing calix[*n*]arenes, where $n \geq 6$.^[3] Moreover, there is even less data on azacalix[*n*]arenes, where the bridge ($-\text{NR}-$) has an addition group (R) bound to the nitrogen which can potentially be varied to control the sterics and/or electronics of the system.^[4] Given this, we have initiated a study of the coordination chemistry of both dimethyloxa- and azacalix[*n*]arenes with a view to investigating their potential as catalysts for the ring opening polymerization (ROP) of cyclic esters. Given recent successes using titanocalix[*n*]arenes for ROP (see Chart 1),^[5] we opted here to focus on titanium-containing dimethyloxa- and azacalixarenes, and have structurally characterized a number of interesting poly-metallic species (see Chart 2). The ability of these

complexes to act as pre-catalysts for the ROP of ϵ -caprolactone (ϵ -CL), δ -valerolactone (δ -VL) and *rac*-lactide (*r*-LA) has been investigated; the copolymerization of ϵ -CL and *r*-LA was also investigated.

Results and Discussion

Syntheses and solid-state structures

Dioxacalix[6]arene complexes

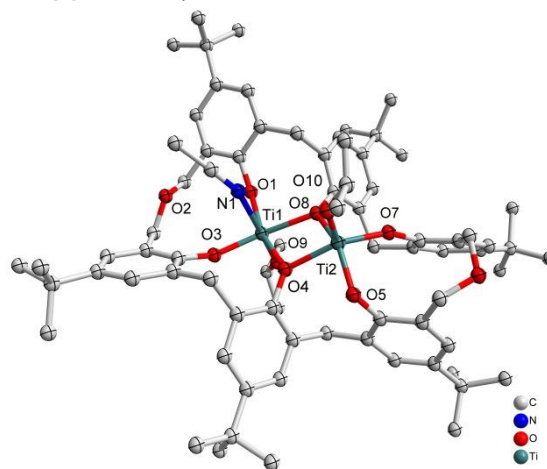


Figure 1. Molecular structure of $[\text{Ti}_2(\text{O}i\text{Pr})_2(\text{MeCN})\text{L}^1]\cdot 3.5\text{MeCN}$ (**1**·3.5MeCN). Solvent molecules and hydrogen atoms omitted for clarity.

^a Plastics Collaboratory, Department of Chemistry, University of Hull, Cottingham Road, Hull, HU6 7RX, UK. E-mail: c.redshaw@hull.ac.uk

^b Collaborative Innovation Center of Atmospheric Environment and Equipment Technology, Jiangsu Key Laboratory of Atmospheric Environment Monitoring and Pollution Control, School of Environmental Science and Engineering, Nanjing University of Information Science & Technology, Nanjing 210044, P. R. China.



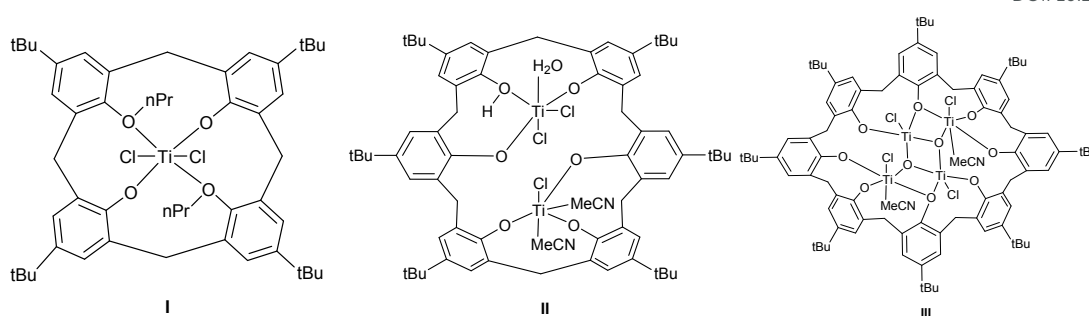


Chart 1. Known calixarene pre-catalysts for the ROP of cyclic esters.

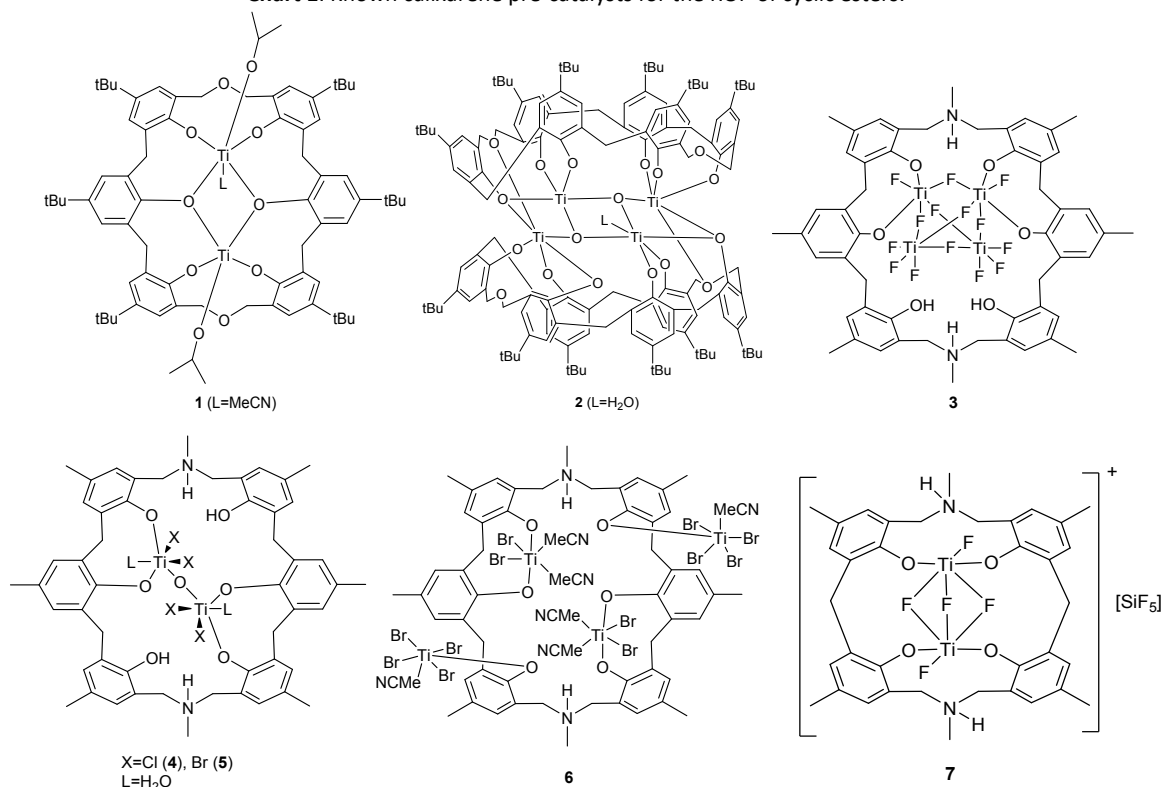


Chart 2. Pre-catalysts prepared herein.

Interaction of an excess (3 equiv.) of $[\text{Ti}(\text{O}i\text{Pr})_4]$ with *p*-*tert*-butyltetrahomodioxacalix[6]arene H_6 (L^1H_6) in refluxing toluene afforded, after work-up (MeCN), the orange complex $[\text{Ti}_2(\text{O}i\text{Pr})_2(\text{MeCN})\text{L}^1] \cdot 3.5\text{MeCN}$ (**1**·3.5MeCN) in 52% yield. The molecular structure is shown in Figure 1, with selected bond lengths and angles given in the ESI; crystallographic data are given in Table 5. The complex contains two titanium centres, one of which, Ti(1), is distorted octahedral bound by an isopropoxide ligand, an acetonitrile ligand and four calixarene phenoxide oxygens in a square plane, two of which are shared with Ti(2). Ti(2) is five-coordinate and adopts a slightly distorted rectangular pyramidal ($\tau = 0.015$).^[6]

If the reaction is conducted in the presence of adventitious oxygen/water and using only two equivalents of $[\text{Ti}(\text{O}i\text{Pr})_4]$, then the isopropoxide groups are lost and a structure involving a titanium-oxygen Ti_4O_4 ladder sandwiched between two oxacalix[6]arenes is formed, namely $[\text{Ti}_4(\mu_3\text{-O})_2(\text{H}_2\text{O})$

(L^1) $_2$]·MeCN (**2**·MeCN). The molecular structure is shown in Figure 2, with selected bond lengths and angles given in the ESI. The water ligand partially occupies positions at Ti(1) and Ti(1#) (50:50). We note that calix[8]arene titanium ladder complexes have recently been isolated and utilized for ROP, CO_2 photoreduction and photocatalytic H_2 production.^[5b, 7]

Azacalixarene complexes

Reaction of *p*-methyl-dimethyldiazacalix[6]arene H_6 (L^2H_6) with four equivalents of $[\text{TiF}_4]$ in refluxing toluene afforded, following work-up (MeCN), the orange complex $[\text{Ti}_4\text{F}_{14}\text{L}^2(\text{H}_2)(\text{H})_2] \cdot 2.5\text{MeCN}$ (**3**·2.5MeCN). The molecular structure is shown in Figure 3, with selected bond lengths and angles given in the ESI. The complex contains four distorted octahedral titanium centres each linked via fluoride bridges to give a central Ti_4F_{14} core. The azacalixarene acts as a bidentate O,O -



chelate to Ti(1) and to Ti(2), leaving two uncoordinated phenolic groups on the macrocycle.

View Article Online
DOI: 10.1039/D1DT00189B

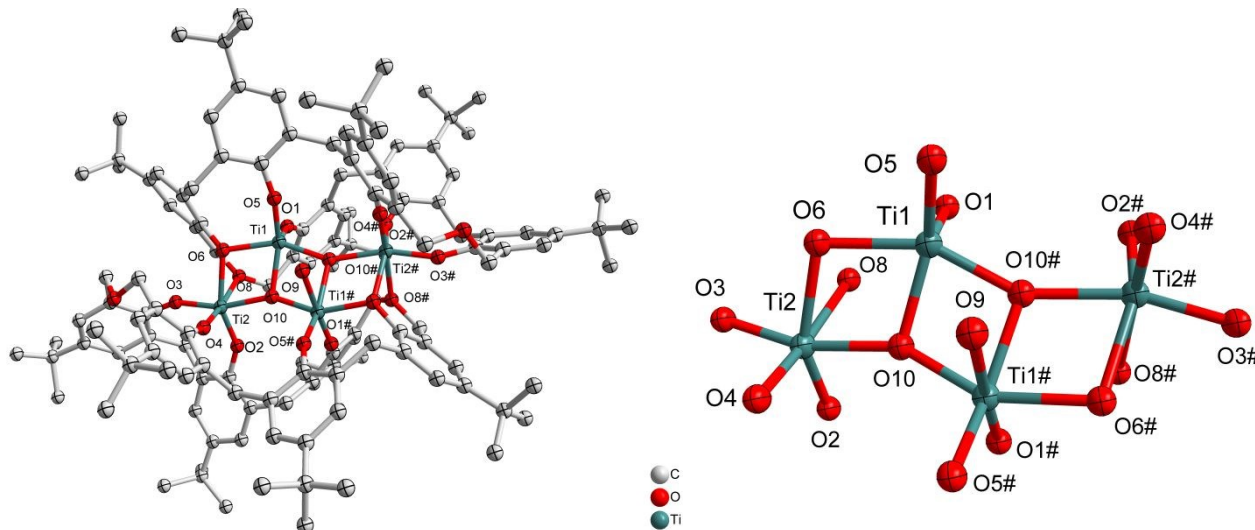


Figure 2. Left: molecular structure of $[Ti_4(\mu_3-O)_2(H_2O)(L^1)_2] \cdot MeCN$ (**2**·MeCN); Right: core of the structure. Solvent molecules and hydrogen atoms omitted for clarity.

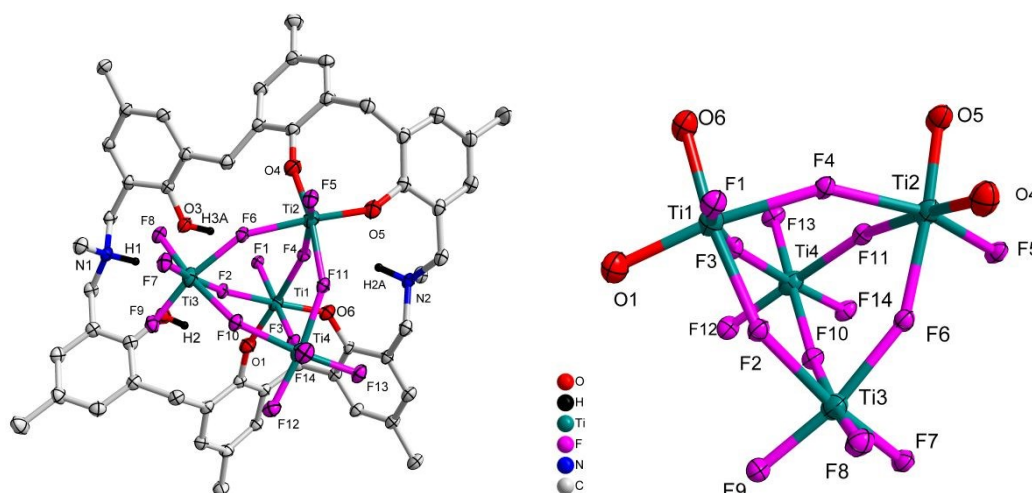


Figure 3. Left: molecular structure of $[Ti_4F_{14}L^2H_2(H_2)] \cdot 2.5MeCN$ (**3**·2.5MeCN); Right: core of the structure. Solvent molecules and hydrogen atoms omitted for clarity.

Treatment of L^2H_6 with two equivalents of $[TiCl_4(THF)_2]$ in refluxing toluene afforded, after work-up (MeCN), dark red prisms of $[Ti_2Cl_4(H_2O)_2OL^2H_2(H_2)] \cdot 5MeCN$ (**4**·5MeCN) in 41% yield. The molecular structure is shown in Figure 4, with selected bond lengths and angles given in the ESI. The complex contains two distorted octahedral titanium centres linked via a near linear oxo bridge $[Ti(1)-O(7)-Ti(2)$ 168.84(6)]. The coordination at each Ti centre is completed by two adjacent phenoxides of the calixarene, a water molecule and two chlorides, one of which is found *trans* to the oxo bridge. The titanium phenoxide bond lengths are typical [1.8324(11) – 1.8975(11) Å], whilst those to the water ligands are, as expected, somewhat longer [2.1445(12) and 2.1570(11) Å].^[5b,8] The overall charge is balanced by the protonated aza bridges of the calixarene.

Similar treatment of L^2H_6 with two equivalents of $[TiBr_4]$ resulted in the isostructural complex $[Ti_2Br_4(H_2O)_2OL^2H_2(H_2)] \cdot 2MeCN$ (**5**·4.5MeCN) in 32% yield. The molecular structure is shown in Figure 5, with selected bond lengths and angles given in the ESI. As in **4**, a linear oxo bridge $[Ti(2)-O(7)-Ti(1)$ 172.65(17)] links the two distorted octahedral centres, and a bromide at each Ti centre can be found *trans* to the μ_2-O . The Ti-O bond length range is similar to that in **4**.



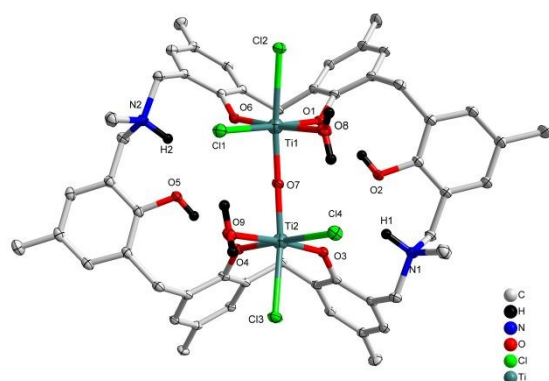


Figure 4. Molecular structure of $[\text{Ti}_2\text{Cl}_4(\text{H}_2\text{O})_2\text{OL}^2\text{H}_2(\text{H})_2]\cdot 5\text{MeCN}$ (**4·5MeCN**). Solvent molecules and hydrogen atoms omitted for clarity.

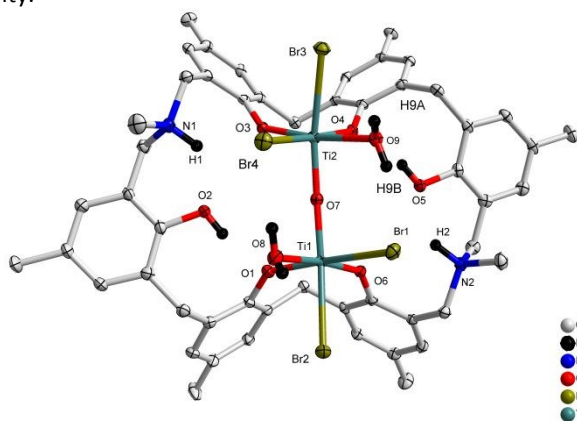


Figure 5. Molecular structure of $[\text{Ti}_2\text{Br}_4(\text{H}_2\text{O})_2\text{OL}^2\text{H}_2(\text{H})_2]\cdot 4.5\text{MeCN}$ (**5·4.5MeCN**). Solvent molecules and hydrogen atoms omitted for clarity.

Reaction of L^2H_6 with excess $[\text{TiBr}_4]$ led to the isolation of the orange complex $[\text{Ti}_4\text{Br}_{12}\text{L}^2(\text{H})_2(\text{MeCN})_6]\cdot 7\text{MeCN}$ (**6·7MeCN**) in 26% isolated yield. A view of the molecular structure is shown in figure 6, with selected bond lengths and angles given in the ESI. The asymmetric unit of **6·7MeCN** contains two independent half molecules each comprising one half a *p*-methyldimethyldiazacalix[6]arene and two Ti ions (Ti1 and Ti2 in first half molecule; Ti3 and Ti4 in second half molecule). The complete molecule in each case is generated by the inversion centre. The two half molecules are similar but are not related by symmetry. In each, the two octahedral Ti ions have different environments. One (Ti1 or Ti3) is coordinated by four bromide ions in a square plane, with O from the calix and NCCH_3 in *trans* arrangement. The calixarene is twisted so that the phenoxide points away from the centre of the molecule and places Ti1 and Ti1_i on opposite sides of the plane of the calixarene (symmop *i* = 1-*x*, -*y*, -*z*). A very similar arrangement is observed for Ti3 and Ti3_{ii} (symm. op. *ii* = 2-*x*, 1-*y*, 1-*z*). The second Ti ion (Ti2 & Ti4) is coordinated in an 8-membered chelate ring, by two geminal phenoxides from the calixarene, two *cis* NCCH_3 in approximately the same plane, and two *trans* bromide ions. The twisted orientation of the calixarene allows for the formation of an N-H...Br hydrogen bond from the protonated aza linkage.

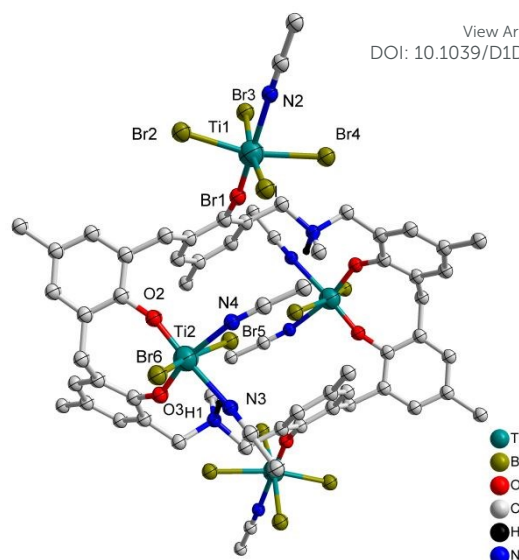


Figure 6. Molecular structure of $[\text{Ti}_4\text{Br}_{12}\text{L}^2(\text{H})_2(\text{MeCN})_6]\cdot 7\text{MeCN}$ (**6·7MeCN**). Solvent molecules and hydrogen atoms omitted for clarity.

When L^2H_6 was treated with four equivalents of $[\text{TiF}_4]$, orange prisms were isolated on work-up, albeit in poor yield (< 20%). A crystal structure determination revealed the complex to be $[\text{Ti}_2\text{F}_2(\mu\text{-F})_3\text{L}^3(\text{H})_2(\text{SiF}_5)]\cdot 2\text{MeCN}$ (**7·2MeCN**), see Figure 7. In **7·2MeCN**, triply bridging fluorides link two distorted octahedral Ti centers, with a terminal fluoride and two adjacent phenoxides of the macrocycle completing the coordination sphere at each metal centre. The SiF_5^- ion is thought to result from the scavenging of HF formed during the reaction. As noted previously, the scavenging of HF can occur via the reaction $5\text{HF} + \text{SiO}_2 \rightarrow 2\text{H}_2\text{O} + \text{H}^+ + \text{SiF}_5^-$.^[9]

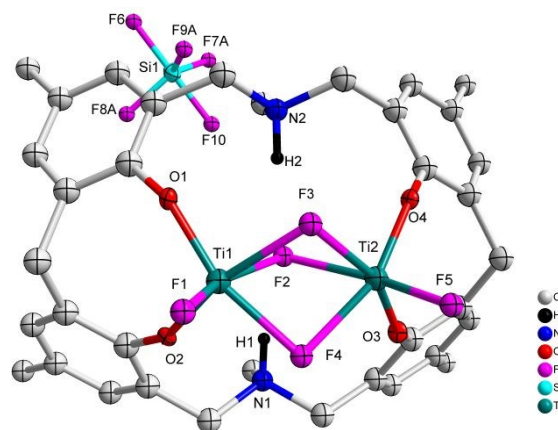


Figure 7. Molecular structure of $[\text{Ti}_2\text{F}_2(\mu\text{-F})_3\text{L}^3(\text{H})_2(\text{SiF}_5)]\cdot 2\text{MeCN}$ (**7·2MeCN**). Solvent molecules and hydrogen atoms omitted for clarity.

Ring opening polymerization studies

General: The performance of these complexes to act as pre-catalysts for the ring opening polymerization (ROP) of ϵ -caprolactone (ϵ -CL), δ -valerolactone (δ -VL) and *rac*-lactide (*r*-LA) with one equivalent of benzyl alcohol (BnOH) per titanium



present, has been investigated. The co-polymerization of ϵ -caprolactone and *rac*-lactide (Table 4) has also been investigated.

ϵ -caprolactone (ϵ -CL)

Complexes 1-7 were screened for their ability to polymerise ϵ -caprolactone and the results are collated in Table 1. The polymerization screening indicated that the best conditions were 250 equivalents of ϵ -caprolactone to titanium at 130 °C. In separate experiments, we re-recorded the ^1H NMR spectra of 1 – 7 after prolonged heating at 130 °C to confirm their stability during the ROP conditions. The activity of complex 1 increased with temperature and peaked at 250 equivalents of monomer. Complex 1 was also active at low catalyst loading leading to 80.4% conversion after 8 h for 1000 equivalents of monomer. All polymers obtained were of relatively low polydispersity (PDI < 1.75), which suggested that these polymerizations occurred without significant side reactions. The M_n were found to be much lower than the calculated values. Interestingly, complex 1 proved to be active also under aerobic conditions achieving 84% conversion during 8 h (Table 1, run 7), which may suggest that the dioxalix[6]arene based complexes 1 and 2 can tolerate air/water during the ROP catalysis.

The screening of complexes 1-7 (Table 1) revealed that the titanium-based L^1 complexes namely 1 and 2 herein, exhibited higher activities than other complexes under the conditions employed. After 24 h (Table 1), complexes 3, 4 and 7 afforded relatively lower conversions (<90%), whereas higher conversions (>90%) were reached using complexes 1, 2, 5 and 6, under similar conditions. From a kinetic study (Figure 8), it was observed that the PCL polymerization rate followed the order: 2>1>5>6>4>3>7. Compared with the larger titanocalix[6]arene complexes (complexes 1-6), complex 7 was found to be relatively inactive (Table 1, run 12 and 22), presumably due to its low solubility in toluene. The observed activity of complex 2 surpassed that of the other

complexes screened herein, and this may be attributed to the arrangement of and distance between the Ti centers. The higher activity of the chloro- (4) and bromo- (5, 6) azacalixarene titanium complexes compared with that of fluoro- (3) compound can be explained considering the lability of the ligands present. This is in line with our recent study on titanocalix[4]arenes, in which the presence of a labile ligand (*i.e.* MeCN and H₂O) proved beneficial for the catalyst activity.^[5] ^1H NMR spectra of the PCL indicated the presence of an BnO end group (e.g. Figure S4, ESI), which agrees with the MALDI-ToF mass spectra (e.g. Figure S1, ESI) and indicates that the polymerization proceeded via a coordination insertion mechanism. Indeed, the MALDI-ToF spectrum of the sample displayed a major series of peaks separated by 114 m/z units accountable to two OH terminated PCL *n*-mers ($M = 17 (\text{OH}) + 1(\text{H}) + n \times 114.14 (\text{CL}) + 22.99 (\text{Na}^+)$) and there is a part of peaks consistent with the polymer terminated by OH and BnO end group ($M = n \times 114.12 (\text{CL}) + 108.05 (\text{BnOH}) + 22.99 (\text{Na}^+)$) and cyclic PCL ($M = n \times 114.12 (\text{CL}) + 22.99 (\text{Na}^+)$).

δ -valerolactone (δ -VL)

Furthermore, complexes 1-7 were also evaluated as pre-catalysts in the presence of one equivalent of BnOH for the ROP of δ -VL (Table 2). Using compound 1, the conditions of temperature and [Ti]: [δ -VL] were varied. On increasing the temperature to 130 °C and lowering the monomer to pre-catalyst ratio, best results were achieved at 130 °C using [Ti]: [δ -VL] at 1:250 over 8 h. As in the case of the ROP of ϵ -CL, kinetic studies (Figure 9) revealed that the catalytic activities followed the order: 2>1>5>6>4>3>7. As for the ROP of ϵ -CL, nearly all observed M_n values were significantly lower than the calculated values. The MALDI-ToF mass spectra (Figure S2, ESI) exhibited a major family of peaks consistent with BnO end groups [$M = 108.05 (\text{BnOH}) + n \times 100.12 (\text{VL}) + 22.99 (\text{Na}^+)$], and a minor family assigned to cyclic PVL. ^1H NMR spectra of the PVL also indicated the presence of an BnO end group (e.g. Figure S5, ESI).

Table 1. ROP of ϵ -CL using 1 – 7.

Run	Cat.	CL: Ti: BnOH	T/°C	t/h	Conv ^a (%)	$M_{n,\text{GPC}} \times 10^{-3b}$	$M_w \times 10^{-3b}$	$M_{n,\text{Cal}} \times 10^{-3c}$	PDI ^d	TON ^f
1	1	1000: 1: 1	130	8	80.4	7.10	9.71	91.98	1.37	804
2	1	500: 1: 1	130	8	84.9	8.44	13.41	48.66	1.59	425
3	1	250: 1: 1	130	8	92.3	10.58	18.43	26.55	1.74	231
4	1	100: 1: 1	130	8	93.4	5.04	6.54	10.87	1.30	93
5	1	250: 1: 1	100	8	74.2	4.87	5.49	21.38	1.13	186
6	1	250: 1: 1	80	8	28.3	2.95	3.43	8.28	1.16	71
7	1 ^e	250: 1: 1	130	8	85.4	9.43	12.03	24.58	1.27	214
8	2	250: 1: 1	130	8	93.5	12.54	15.20	26.89	1.21	234
9	3	250: 1: 1	130	8	62.3	4.37	6.43	17.99	1.47	156
10	4	250: 1: 1	130	8	67.5	6.19	9.97	19.47	1.50	169
11	5	250: 1: 1	130	8	77.1	8.21	12.32	22.21	1.61	193
12	6	250: 1: 1	130	8	84.2	8.84	13.09	24.10	1.48	211
13	7	250: 1: 1	130	8	25.3	-	-	-	-	63
14	1	250: 1: 1	130	24	>99	11.43	16.32	28.46	1.42	248



ARTICLE

Journal Name

15	2	250: 1: 1	130	24	>99	13.34	23.14	28.46	1.73	248
16	3	250: 1: 1	130	24	76.4	6.78	7.93	22.01	1.17	191
17	4	250: 1: 1	130	24	82.5	8.40	11.11	23.75	1.32	206
18	5	250: 1: 1	130	24	96.4	8.28	11.64	27.72	1.41	241
19	6	250: 1: 1	130	24	>99	10.04	15.82	28.46	1.58	248
20	7	250: 1: 1	130	24	34.6	2.28	2.63	9.98	1.15	87
21	1	250: 1: 0	130	24	71.6	4.30	5.20	20.49	1.20	179
22	2	250: 1: 0	130	24	74.7	6.13	7.01	21.37	1.14	187
23	3	250: 1: 0	130	24	59.1	2.38	3.62	16.92	1.52	148
24	4	250: 1: 0	130	24	63.8	3.42	5.51	18.26	1.61	160
25	5	250: 1: 0	130	24	69.2	4.18	5.79	19.80	1.39	173
26	6	250: 1: 0	130	24	62.8	4.85	5.78	17.97	1.19	157
27	7	250: 1: 0	130	24	-	-	-	-	-	-

^a Determined by ¹H NMR spectroscopy. ^b $M_{n,w}$, GPC values corrected considering Mark–Houwink factor (0.56) from polystyrene standards in THF. ^c Calculated from $([\text{monomer}]_0/\text{Ti}) \times \text{conv} (\%) \times \text{monomer molecular weight } (M_{\text{CL}}=114.14) + \text{Molecular weight of BnOH}$. ^d From GPC. ^e Reaction performed in air. ^f Turnover number (TON) = number of moles of ϵ -CL consumed/ number of moles Ti.

Table 2. ROP of δ -VL using using 1 – 7.

Run	Cat.	VL: Ti: BnOH	T/°C	t/h	Conv ^a (%)	$M_{n,\text{GPC}} \times 10^{-3b}$	$M_w \times 10^{-3b}$	$M_{n,\text{Cal}} \times 10^{-3c}$	PDI ^d	TON ^f
1	1	1000: 1: 1	130	8	81.2	11.56	18.23	81.30	1.58	812
2	1	500: 1: 1	130	8	80.1	12.27	17.54	40.10	1.43	401
3	1	250: 1: 1	130	8	89.4	13.49	27.46	22.38	2.03	224
4	1	100: 1: 1	130	8	86.7	5.84	8.12	8.68	1.38	87
5	1	250: 1: 1	100	8	68.1	4.06	4.67	17.05	1.15	170
6	1	250: 1: 1	80	8	-	-	-	-	-	-
7	1 ^e	250: 1: 1	130	8	74.6	10.23	14.56	18.67	1.42	187
8	2	250: 1: 1	130	8	90.8	16.44	32.07	22.73	1.95	227
9	3	250: 1: 1	130	8	64.6	6.36	8.02	16.17	1.26	162
10	4	250: 1: 1	130	8	70.3	7.10	9.71	17.60	1.36	176
11	5	250: 1: 1	130	8	83.3	9.58	14.59	20.85	1.52	208
12	6	250: 1: 1	130	8	80.6	10.76	15.96	20.28	1.48	202
13	7	250: 1: 1	130	8	38.1	2.64	3.24	9.54	1.22	95

^a Determined by ¹H NMR spectroscopy. ^b $M_{n,w}$, GPC values corrected considering Mark–Houwink factor (0.57) from polystyrene standards in THF. ^c Calculated from $([\text{monomer}]_0/\text{Ti}) \times \text{conv} (\%) \times \text{monomer molecular weight } (M_{\text{VL}}=100.16) + \text{Molecular weight of BnOH}$. ^d From GPC. ^e Reaction performed in air. ^f Turnover number (TON) = number of moles of δ -VL consumed/ number of moles Ti.

Table 3. ROP of *rac*-lactide using complexes 1– 7.

Run	Cat.	LA: Ti: BnOH	T/°C	t/h	Conv ^a (%)	$M_{n,\text{GPC}} \times 10^{-3b}$	$M_w \times 10^{-3b}$	Pr^c	$M_{n,\text{Cal}} \times 10^{-3d}$	PDI ^e	TON ^f
1	1	250: 1: 1	130	24	75.4	5.98	10.27	0.52	27.16	1.72	189
2	2	250: 1: 1	130	24	78.1	7.32	8.23	0.40	28.14	1.12	195
3	3	250: 1: 1	130	24	36.9	5.86	8.75	0.58	13.29	1.49	92
4	4	250: 1: 1	130	24	54.3	5.10	7.57	0.39	19.56	1.43	136
5	5	250: 1: 1	130	24	59.1	4.98	7.02	0.46	21.29	1.41	148
6	6	250: 1: 1	130	24	62.6	4.38	5.39	0.41	22.66	1.05	157
7	7	250: 1: 1	130	24	25.6	3.46	4.86	0.42	9.33	1.18	64

^a Determined by ¹H NMR spectroscopy on crude reaction mixture. ^b $M_{n,w}$, GPC values corrected considering Mark–Houwink factor (0.58) from polystyrene standards in THF. ^c From 2D *J*-resolved ¹H NMR spectroscopy. ^d Calculated from $([\text{Monomer}]_0/\text{Ti}) \times \text{conv} (\%) \times \text{Monomer molecular weight } (M_{\text{LA}}=144.13) + \text{Molecular weight of BnOH}$. ^e From GPC. ^f Turnover number (TON) = number of moles of *r*-LA consumed/ number of moles Ti.



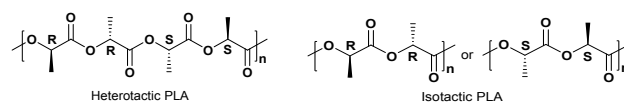
Table 4. ROP of co-polymer (*r*-LA + ϵ -CL) using 1-7.

Run ^a	Cat.	LA: CL: Ti: BnOH	t/h	T/ $^{\circ}$ C	Conv ^b (%)	$M_{n,GPC} \times 10^{-3,c,d}$	$M_w \times 10^{-3,c,d}$	PDI ^c
1	1	250:250:1:1	130	24	80.2	14.16	26.71	1.88
2	2	250:250:1:1	130	24	85.1	16.44	32.07	1.95
3	3	250:250:1:1	130	24	72.4	9.48	14.23	1.50
4	4	250:250:1:1	130	24	75.9	10.63	17.37	1.63
5	5	250:250:1:1	130	24	82.7	14.42	21.98	1.52
6	6	250:250:1:1	130	24	80.1	15.01	22.88	1.52
7	7	250:250:1:1	130	24	33.8	2.35	2.75	1.16

^a Testing method: *rac*-lactide was firstly added and heating for 24 h, then ϵ -caprolactone was added and heating for 24 h. ^b Determined by ¹H NMR spectroscopy on crude reaction mixture based on ϵ -CL. ^c From GPC. ^d M_n values were determined by GPC in THF vs. PS standards and were corrected with a Mark-Houwink factor $M_{n/w} GPC = [(M_{n/w} \text{ measured} \times 0.56 \times (1-\%CL) + M_{n/w} \text{ measured} \times 0.58 \times (1-\%LA))]$.

ROP of *r*-lactide

Selected complexes were also employed as pre-catalysts in the ROP of *r*-LA (Table 3). Best conversion was achieved in the presence of 2 (78.1%, run 2). The M_n of the polymer was lower than the calculated value albeit with narrow molecular weight distribution (7320 and 1.12, respectively). In the case of systems 1-7, all polymers obtained were of low polydispersity (PDI < 1.75), which suggested that there was reasonable control for polymerization. However, 7 only allowed for 25.6% monomer conversion affording low molecular weight species. ¹H NMR spectra of the PLA indicated the presence of a BnO end group (e.g. Figure S6, ESI), which agrees with the MALDI-ToF mass spectra (e.g. Figure S3, ESI). The sample was analysed by MALDI-ToF mass spectra in positive-linear mode, the expected series corresponding to repeating unit mass of 72/144 for half/full LA was observed and the polymer chain was terminated by OH and BnO end group [$M = 108.05$ (BnOH) + $n \times 72.06$ (C₃H₄O₂) + 22.99 (Na⁺)]. The syndiotactic bias was determined by 2D *J*-resolved ¹H NMR spectroscopy, investigating the methine area (5.13-5.20 ppm) of the spectra (e.g. Figure. S8, ESI).^[10] The peaks were assigned to the corresponding tetrads according to the literature.^[10] For *rac*-lactide, when $P_r=0.5$, the afforded PLA is an atactic polymer, and when $P_r=0$, an isotactic polymer. The observed values herein ($P_r=0.39-0.52$) suggested the catalysts afforded almost heterotactic polymers (Chart 3).

**Chart 3.** Microstructure of heterotactic and isotactic poly(*rac*-lactide).^[11]

Co-polymerization of *r*-LA and ϵ -CL

The co-polymerization of *r*-LA and ϵ -CL was next investigated (Table 4). The complexes exhibited moderate conversions, with complex 2 performing best (85.1%), and with 1 and 3-6 also producing conversions > 70%. In general, the systems appeared to be relatively well behaved with PDIs in the range 1.16-1.95; ¹H NMR spectra were consistent with the presence of BnO and OH end groups (Figure S7, ESI). The composition of the copolymer was further investigated by ¹³C NMR spectroscopy. In fact, diagnostic resonances belonging to CL-CL-CL, LA-CL-CL, CL-CL-LA, LA-CL-LA, LA-LA-CL, CL-LA-LA and LA-LA-LA dyads can be observed in the region between δ 173.6 and 169.6 ppm (Figure S9, ESI). Based on the current results, the number-average sequence length was found to be 1.18 and 5.10 for CL and LA, respectively (Figure S9, Equations 1-2, ESI). Furthermore, no peaks corresponding to the CL-LA-CL triad at 171.1 ppm was observed. Such signals arise from the transesterification of the cleavage of the lactyl-lactyl bond in the lactidyl unit.^[12]

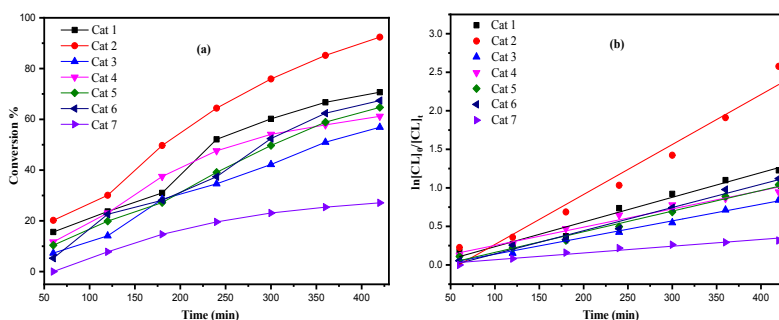


Figure 8. (a) Relationship between conversion and time for the polymerization of ϵ -CL by using complex **1-7**; (b) Plot of $\ln[\text{CL}]_0/[\text{CL}]_t$ vs. time for the polymerization of ϵ -CL by using complexes **1-7**; Conditions: $T=130^\circ\text{C}$, $n_{\text{Monomer}}: n_{\text{Ti}}: \text{BnOH}=250:1:1$. DOI: 10.1039/D1DT00189B

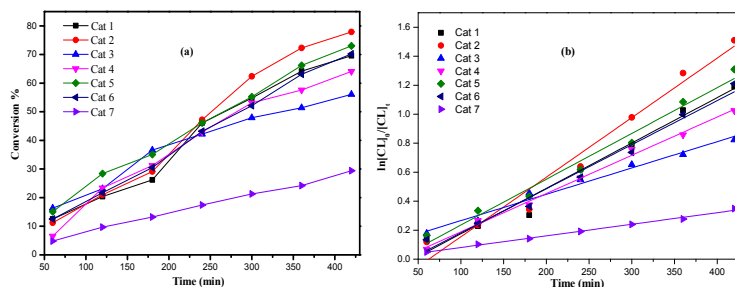


Figure 9. (a) Relationship between conversion and time for the polymerization of δ -VL by using complex **1-7**; (b) Plot of $\ln[\text{VL}]_0/[\text{VL}]_t$ vs. time for the polymerization of δ -VL by using complexes **1-7**; Conditions: $T=130^\circ\text{C}$, $n_{\text{Monomer}}: n_{\text{Ti}}: \text{BnOH}=250:1:1$.

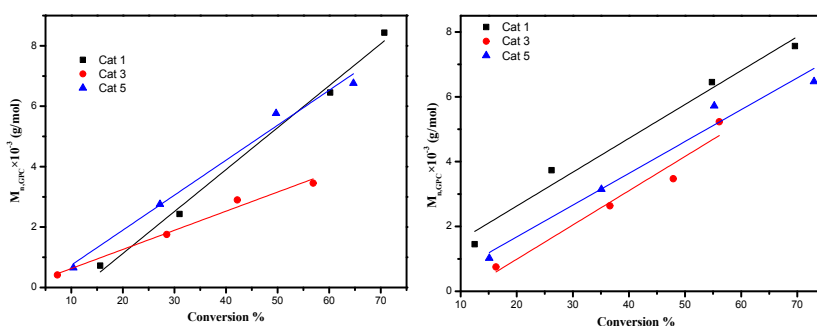


Figure 10. Left: M_n vs. monomer conversion in the ROP of ϵ -CL by using **1, 3** and **5**; Right: M_n vs. monomer conversion in the ROP of δ -VL by using **1, 3** and **5**; Conditions: $T=130^\circ\text{C}$, $n_{\text{Monomer}}: n_{\text{Ti}}: \text{BnOH}=250:1:1$.

Kinetics

From a kinetic study of the ROP of ϵ -CL using **1-7**, it was observed that the polymerization rate exhibited first-order dependence on the ϵ -CL concentration (Figure 8(a)), and the conversion of monomer achieved over 420 min was >25%. The activity trend in this case revealed that **2** was the most active and then $1>5>6>4>3>7$. An induction period of 2 hours observed for complexes **1-6** could be ascribed to the longer time required for the formation of the catalytically active species. A similar result was also observed in the polymerization of δ -VL (Figure 9).

The dependence of the M_n and molecular weight distribution on the monomer conversion in the reactions catalyzed by **1, 3, 5** with BnOH was also investigated (Figure 10). For the ROP of ϵ -CL, the polymer M_n was shown to increase linearly with the conversion, which suggested that the polymerization was well controlled (Figure 10, left). A similar outcome was also observed in the reaction involving δ -VL (Figure 10, right).

ROP of ω -pentadecalactone

To enhance the thermal properties of the polymers obtained herein, we also investigated the ROP of the ω -pentadecalactone. Unfortunately, none of the systems herein

proved to be effective as catalysts for the ROP of ω -pentadecalactone either in solution at high temperatures (130°C) or as melts.

Conclusions

In this work, we report rare examples of metal (here titanium) complexes of larger dioxacalix[6]arenes and extend the work to include even rarer examples of titanium complexes bearing azacalixarenes. The molecular structures reveal how these macrocycles can support multiple metal centres which adopt some interesting structural motifs. The complexes are active for the ring opening polymerization of ϵ -caprolactone (ϵ -CL), δ -valerolactone (δ -VL) and *rac*-lactide (*r*-LA) but not ω -pentadecalactone. In all cases, the oxo complex $[\text{Ti}_4\text{O}_4(\text{L}^1)_2] \cdot \text{MeCN}$ (**2**·MeCN) proved to be the most active with first order kinetics.

Experimental

General

All reactions were conducted under an inert atmosphere using standard Schlenk techniques. Toluene was dried from sodium, acetonitrile was distilled from calcium hydride, diethylether was



distilled from sodium benzophenone, and all solvents were degassed prior to use. The dioxacalix[6]arene and azacalixarenes were prepared according to the literature methods.^[13] All other chemicals were purchased from commercial sources. IR spectra (nujol mulls, KBr windows) were recorded on a Nicolet Avatar 360 FT IR spectrometer; ¹H NMR spectra were recorded at room temperature on a Varian VXR 400 S spectrometer at 400 MHz or a Gemini 300 NMR spectrometer or a Bruker Advance DPX-300 spectrometer at 300 MHz. The ¹H NMR spectra were calibrated against the residual protio impurity of the deuterated solvent. Elemental analyses were performed by the elemental analysis service at the University of Hull. Matrix Assisted Laser Desorption/Ionization Time of Flight (MALDI-TOF) mass spectrometry was performed in a Bruker autoflex III smart beam in linear mode, and the spectra were acquired by averaging at least 100 laser shots. 2,5-Dihydroxybenzoic acid was used as the matrix and THF as solvent. Sodium chloride was dissolved in methanol and used as the ionizing agent. Samples were prepared by mixing 20 μl of matrix solution in THF (2 mg·mL⁻¹) with 20 μL of matrix solution (10 mg·mL⁻¹) and 1 μL of a solution of ionizing agent (1 mg·mL⁻¹). Then 1 mL of these mixtures was deposited on a target plate and allowed to dry in air at ambient temperature.

Synthesis of [Ti₂(OiPr)₂(MeCN)L¹]₂·3.5MeCN (1·3.5MeCN).

To [Ti(OiPr)₄] (0.43 g, 1.50 mmol) and L¹H₆ (0.50 g, 0.49 mmol) was added toluene (30 mL) and then the system was refluxed for 12 h. On cooling, the volatiles were removed *in vacuo*, and the residue was extracted into warm MeCN (30 mL). On prolonged standing at 0 °C, an orange crystalline material formed (Figure S10, ESI), yield 0.32 g, 52%. Anal. Cald for C₈₂H₁₀₈N₄O₁₀Ti₂ (sample dried *in-vacuo* for 12 h, -3.5MeCN): C, 71.60; H, 7.06; found C, 71.92; H, 7.28%. IR (nujol mull, KBr): 3231w, 2923s, 2853s, 2349w, 1641.9w, 1461m, 1413w, 1377m, 1303w, 1260s, 1212w, 1092s, 1019s, 863w, 799s. ¹H NMR (CDCl₃) δ: 6.86-7.32 (m, 12H, arylH), 5.44 (m, 2H, -OCH(CH₃)₂), 5.04-5.21 (m, 4H, -OCH₂-), 4.87 (d, J=4.8 Hz, 4H, -OCH₂-), 4.48 (m, 4H, -CH₂-), 3.40 (d, J=12.4 Hz, 4H, -CH₂-), 2.03 (s, 3H, MeCN), 1.56 (m, 12H, -OCH(CH₃)₂), 2.03 (s, 3H, MeCN) 1.21-1.34 (m, 54H, -C(CH₃)₃). Mass Spec (EI): 1267.6 [M+Na⁺-3.5MeCN].

Synthesis of [Ti₄(μ₃-O)₂(H₂O)(L¹)₂]₂·MeCN (2·MeCN).

As for **1**, but using [Ti(OiPr)₄] (0.29 g, 1.00 mmol) and L¹H₆ (0.50 g, 0.49 mmol) affording **2** as orange prisms. Single orange prisms were grown from a saturated MeCN (30 mL) solution at 0 °C (yield 0.25 g, 44%). Anal. Cald for C₁₃₅H₁₆₄O₁₈Ti₄ (sample dried *in-vacuo* for 12 h, -MeCN): C, 71.54; H, 7.29; found C, 71.91; H, 7.38%; IR (nujol mull, KBr): 2726w, 2359w, 2340w, 1651w, 1463s, 1377s, 1301m, 1260m, 1209m, 1080m, 1020m, 941w, 926w, 899w, 899m, 798s. ¹H NMR (CDCl₃) δ: 6.89-7.32 (m, 12H, arylH), 5.36 (d, J=6.8 Hz, 4H, -OCH₂-), 5.02-5.17 (m, 4H, -OCH₂-), 4.88 (d, d, J=6.8 Hz, 4H, -OCH₂-), 4.64 (d, J=6.8 Hz, 4H, -OCH₂-), 4.34 (m, 4H, -CH₂-), 3.49-3.87 (m, 8H, -CH₂-), 2.01 (s, 3H, MeCN), 1.13-1.36 (m, 108H, -C(CH₃)₃). Mass Spec (EI): 2292 [M].

Synthesis of [Ti₄F₁₄L²H₂(H)₂]₂·2.5MeCN (3·2.5MeCN).

As for **1**, but using [TiF₄] (0.31 g, 2.48 mmol) and L²H₆ (0.50 g, 0.62 mmol) affording **3** as red prisms. Single orange prisms were grown from a saturated MeCN (30 mL) solution at room temperature (yield 0.44 g, 56%). Anal. Cald for C₅₂H₅₆F₁₄N₂O₆Ti₄ (sample dried *in-vacuo* for 12 h, -2.5MeCN): C, 49.47; H, 4.47; N, 2.22%. Found C, 50.03; H, 4.85; N, 2.06%. IR (nujol mull, KBr): 3849w, 3435s, 1737w, 1692w, 1552w, 1536s, 1461m, 1383m, 1260s, 1220w, 1093s, 1020s, 928w, 866m, 800m, 688m. ¹H NMR (CDCl₃) δ: 6.98-7.50 (m, 12H, arylH), 3.48-3.73 (m, 8H, -CH₂-), 3.22-3.42 (m, 8H, -NCH₂-), 2.34 (s, 6H, -NCH₃), 2.05-2.18 (m, 18H, -CH₃). ¹⁹F NMR (CDCl₃) δ: -110.18 (bs, 6F), -98.32 (bs, 6F), -69.12 (bs, 2F). Mass Spec (EI): 1283 [M+Na⁺-2.5MeCN].

Synthesis of [Ti₂Cl₄(H₂O)₂OL²H₂(H)₂]₂·4.5MeCN (4·5MeCN).

As for **1**, but using [TiCl₄(THF)₂] (0.41 g, 1.24 mmol) and L²H₆ (0.50 g, 0.62 mmol) affording **4** as dark red prisms. Single orange prisms were grown from a saturated MeCN (30 mL) solution at room temperature (yield 0.28 g, 41%). Anal. Cald for C₅₂H₆₀Cl₄N₂O₉Ti₂ (sample dried *in-vacuo* for 12 h, -5MeCN): C, 57.06; H, 5.53; N, 2.56%. Found C, 56.39; H, 5.25; N, 2.26%. IR (nujol mull, KBr): 3428m, 2745w, 2365w, 2278m, 1705m, 1628w, 1425s, 1357s, 1325m, 1232m, 1029s, 1015w, 799m, 754s. ¹H NMR (CDCl₃) δ: 6.88-7.49 (m, 12H, arylH), 3.71 (d, J=4.8 Hz, 8H, -CH₂-), 3.56 (d, J=4.8 Hz, 8H, -NCH₂-), 2.34 (s, 6H, -NCH₃), 2.00-2.26 (m, 18H, -CH₃), 1.53 (s, 2H, H₂O). Mass Spec (EI): 1053 [M-2H₂O-5MeCN].

Synthesis of [Ti₂Br₄(H₂O)₂OL²H₂(H)₂]₂·4.5MeCN (5·4.5MeCN).

As for **1**, but using [TiBr₄] (0.46 g, 1.24 mmol) and L²H₆ (0.50 g, 0.62 mmol) affording **5** as dark orange prisms. Single orange prisms were grown from a saturated MeCN (30 mL) solution at room temperature (yield 0.25 g, 32%). Anal. Cald for C₅₄H₆₃Br₄N₂O₉Ti₂ (sample dried *in-vacuo* for 12 h, -3.5MeCN): C, 49.38; H, 4.83; N, 3.20%. Found C, 49.62; H, 5.03; N, 2.86%. IR (nujol mull, KBr): 3427m, 2729w, 2348w, 2285m, 2248w, 1605m, 1461s, 1377s, 1302w, 1260s, 1156w, 1039m, 1021m, 863m, 800s. ¹H NMR (CDCl₃) δ: 6.80-7.38 (m, 12H, arylH), 3.79 (m, 8H, -CH₂-), 3.52 (m, 8H, -NCH₂-), 2.30 (s, 6H, -NCH₃), 2.05-2.23 (m, 18H, -CH₃), 1.51 (s, 2H, H₂O). Mass Spec (EI): 1274 [M-4.5MeCN].

Synthesis of [Ti₄Br₁₂L²(H)₂(MeCN)₆]₂·7MeCN (6·7MeCN).

As for **1**, but using [TiBr₄] (1.00 g, 2.69 mmol) and L²H₆ (0.50 g, 0.62 mmol) affording **6** as orange/red prisms. Single orange prisms were grown from a saturated MeCN (30 mL) solution at 0 °C (yield 0.34 g, 26.0%). Anal. Cald for C₆₀H₆₆Br₁₂N₆O₆Ti₄ (sample dried *in-vacuo* for 24h, -3MeCN): Anal. Cald for C, 34.03 H, 3.14; N, 3.97%. Found: C, 33.59 H, 3.10; N, 4.42%. IR (nujol mull, KBr): 2957s, 2852s, 2727w, 2350w, 2283w, 1693w, 1645m, 1567w, 1456s, 1377s, 1308w, 1259m, 1094m, 1019m, 927w, 856m, 800s. ¹H NMR (CD₂Cl₂) δ: 7.24-6.81 (m, 12H, arylH), 3.91 (m, 8H, -CH₂-), 3.41 (m, 8H, -NCH₂-), 2.88 (s, 6H, -NCH₃), 2.24 (m, 18H, -CH₃), 1.95 (s, 12H, MeCN).

Synthesis of [Ti₂F₂(μ-F)₃L³(H)₂(SiF₅)₂]₂·2MeCN (7·2MeCN).

As for **1**, but using [TiF₄] (0.44 g, 3.53 mmol) and L²H₄ (0.50 g, 0.88 mmol) affording **7** as orange/red prisms. Single orange prisms were grown from a saturated MeCN (30 mL) solution at 0 °C (yield 0.15 g, 17%). Anal. Cald for C₃₆H₄₀F₁₀N₂SiO₄Ti₂ (sample dried *in-vacuo* for



12h, -2MeCN): Anal. Calcd for C, 49.22 H, 4.59; N, 3.19%. Found C, 49.82; H, 5.03; N, 3.59%. IR (nujol mull, KBr): 3353w, 2729w, 2360m, 2340w, 2251w, 1606w, 1463s, 1377s, 1304w, 1260m, 1231m, 1162w, 1093m, 1019m, 945w, 927w, 870m, 801m. ¹H NMR (CDCl₃) δ: 6.98-7.50 (m, 8H, arylH), 3.72 (m, 4H -CH₂-), 3.46 (m, 8H, -NCH₂-), 2.34(s, 6H, -CH₃) 1.99 (s, 12H, -NCH₃). ¹⁹F NMR (CDCl₃) δ: -107.27 (bs, 5F), -82.16 (bs, 3F), -72.06 (bs, 2F). Mass Spec (EI): 879 [M-2MeCN].

Procedure for ROP of ε-caprolactone, δ-valerolactone and rac-lactide

A toluene solution of pre-catalyst (0.010 mmol, 1.0 mL toluene) was added into a Schlenk tube in the glove-box at room temperature. The solution was stirred for 2 min, and then the appropriate equivalent of BnOH (from a pre-prepared stock solution of 1 mmol BnOH in 100 mL toluene) and the appropriate amount of ε-CL, δ-VL or r-LA along with 1.5 mL toluene was added to the solution. The reaction mixture was then placed into an oil/sand bath pre-heated at 130 °C, and the solution was stirred for the prescribed time (8 or 24 h). The polymerization mixture was quenched on addition of an excess of glacial acetic acid (0.2 mL) into the solution, and the resultant solution was then poured into methanol (200 mL). The resultant polymer was then collected on filter paper and was dried *in-vacuo*.

Kinetic studies

The polymerizations were carried out at 130 °C in toluene (2 mL) using 0.010 mmol of complex. The molar ratio of monomer to

initiator to co-catalyst was fixed at 250:1:1, and at appropriate time intervals, 0.5 μL aliquots were removed (under N₂) and were quenched with wet CDCl₃. The percent conversion of monomer to polymer was determined using ¹H NMR spectroscopy.

X-ray Crystallography

In all cases, crystals suitable for an X-ray diffraction study were grown from a saturated MeCN solution at either ambient temperature or 0 °C. Single crystal X-ray diffraction data (except **5**) were collected at the UK National Crystallography service using Rigaku Oxford Diffraction ultra-high intensity instruments employing modern areas detectors. X-ray diffraction data for **5**-4.5MeCN were collected using a stoe ipds2 image plate diffractometer operating with molybdenum radiation. In all cases standard procedures were employed for integration and processing of data.

Crystal structures were solved using dual space methods implemented within SHELXT.^[14] Completion of structures was achieved by performing least squares refinement against all unique F² values using SHELXL-2018.^[15] All non-H atoms were refined with anisotropic displacement parameters. Hydrogen atoms were placed using a riding model. Where the location of hydrogen atoms was obvious from difference Fourier maps, C-H and O-H bond lengths were refined subject to chemically sensible restraints. Minor disorder was treated using standard methods.

SQUEEZE^[16] was used to model the disordered solvent in structures **1**, **3**, **4**, **5** and **6**.

Crystallography

Table 5. Crystal structure data for **1**-3.5MeCN, **2**-MeCN, **3**-2.5MeCN, **4**-5MeCN, **5**-4.5MeCN, **6**-7MeCN, **7**-2MeCN.

Compound	1 -3.5MeCN	2 -MeCN	3 -2.5MeCN	4 -5MeCN
Formula	C ₈₃ H _{109.5} N _{4.5} O ₁₀ Ti ₂	C ₁₃₇ H ₁₆₇ NO ₁₈ Ti ₄	C ₅₇ H _{63.5} F ₁₄ N _{4.5} O ₆ Ti ₄	C ₆₂ H ₇₅ Cl ₄ N ₇ O ₉ Ti ₂
Formula weight	1426.04	2307.30	1365.14	1299.86
Crystal system	Monoclinic	Monoclinic	Monoclinic	Triclinic
Space group	P 2 ₁ /c	C 2/c	P 2 ₁ /c	P-1
Unit cell dimensions				
<i>a</i> (Å)	12.0347(2)	28.1243(7)	16.1213(2)	12.6749(8)
<i>b</i> (Å)	28.3198(4)	17.7721(4)	22.8130(2)	14.5410(8)
<i>c</i> (Å)	24.5367(3)	31.2326(9)	17.0185(2)	18.7696(10)
<i>α</i> (°)	90	90	90	111.979
<i>β</i> (°)	103.2370(10)	113.009(3)	102.381(10)	95.829
<i>γ</i> (°)	90	90	90	96.158
<i>V</i> (Å ³)	8140.4(2)	14369.0(7)	6113.42(12)	3151.55(3)
<i>Z</i>	4	4	4	2
Temperature (K)	100(2)	100(2)	100(2)	100(2)
Wavelength (Å)	1.54184	1.54178	1.54178	1.54178
Calculated density	1.147	1.061	1.416	1.240
Absorption coefficient	2.112	2.275	5.091	4.142
Transmission factors	0.69725 and 1.0000	0.52429 and 1.000	0.6143 and 1.0000	0.679 and 1.0000
Crystal size (mm ³)	0.200 × 0.120 × 0.040	0.160 × 0.030 × 0.010	0.150 × 0.080 × 0.050	0.090 × 0.060 × 0.020
<i>θ</i> (max) (°)	66.6	66.5	70.4	68.2
Reflections measured	75678	46013	55482	134309
Unique reflections	14383	12487	11396	11490



Journal Name

ARTICLE

R_{int}	0.0521	0.0985	0.0415	0.0270
Reflections with $F^2 >$	12259	7981	9829	11030
Number of parameters	870	697	741	701
$R_1 [F^2 > 2\sigma(F^2)]$	0.117	0.085	0.063	0.031
wR_2 (all data)	0.368	0.234	0.178	0.091
GOOF, S	1.675	1.024	1.016	1.050
Largest difference	1.961 and -0.795	0.768 and -0.381	1.500 and -0.511	0.831 and -0.376
Compound	5·4.5MeCN	6·7MeCN	7·2MeCN	
Formula	$\text{C}_{61}\text{H}_{73.5}\text{Br}_4\text{N}_{6.5}\text{O}_9\text{Ti}_2$	$\text{C}_{78}\text{H}_{93}\text{Br}_{12}\text{N}_{15}\text{O}_6\text{Ti}_4$	$\text{C}_{40}\text{H}_{46}\text{F}_{10}\text{N}_4\text{O}_4\text{SiTi}_2$	
Formula weight	1457.15	2487.02	960.70	
Crystal system	Triclinic	Triclinic	Triclinic	
Space group	P-1	P-1	P-1	
Unit cell dimensions				
a (Å)	12.8059(9)	17.7979(2)	8.8857(4)	
b (Å)	14.7294(9)	18.1314(1)	13.0733(5)	
c (Å)	18.6847(13)	18.4582(2)	18.4231(11)	
α (°)	111.546(5)	71.110(1)	84.872(4)	
β (°)	94.299(6)	74.116(1)	82.208(4)	
γ (°)	96.876(5)	66.857(1)	73.277(4)	
V (Å ³)	3227.4(4)	5108.21(10)	2027.83(18)	
Z	2	1	2	
Temperature (K)	150(2)	100(2)	100(2)	
Wavelength (Å)	0.71073	1.54178	0.71075	
Calculated density	1.394	1.549	1.573	
Absorption coefficient	2.775	8.449	0.517	
Transmission factors	0.825 and 0.625	1.0000 and 0.66859	1.0000 and 0.20966	
Crystal size (mm ³)	0.360 x 0.260 x 0.200	0.120 x 0.080 x 0.050	0.100 x 0.060 x 0.020	
ϑ (max) (°)	26.373	68.236	27.529	
Reflections measured	25790	237393	14106	
Unique reflections	13079	18616	14106	
R_{int}	0.0792	0.0693	0.1992	
Reflections with $F^2 >$	8355	18616	10493	
Number of parameters	699	986	547	
$R_1 [F^2 > 2\sigma(F^2)]$	0.0458	0.0662	0.105	
wR_2 (all data)	0.1066	0.1895	0.2964	
GOOF, S	0.859	1.021	1.026	
Largest difference	0.894 and -0.841	1.542 and -1.156	2.991 and -0.829	

Electronic supplementary information (ESI) available. CCDC 2057320–2057326 (1·3.5MeCN, 2·MeCN, 3·2.5MeCN, 4·5MeCN, 5·4.5, 6·7MeCN, 7·2MeCN) contain the supplementary crystallographic data. For ESI and crystallographic data in CIF or other electronic format see DOI:

We thank the China Scholarship Council (CSC) for a PhD Scholarship to TX. The EPSRC Mass Spectrometry Service (Swansea, UK) and the EPSRC National X-ray Crystallography Service (Southampton) are thanked for data collection. CR also thanks the EPSRC (grant EP/S025537/1) for financial support.

Conflicts of interest

There are no conflicts to declare.

Acknowledgements

References

- [1] (a) D. H. Homden and C. Redshaw, *Chem. Rev.*, 2008, **108**, 5086–5130; (b) Coordination Chemistry and Applications of Phenolic Calixarene–metal Complexes. Y. Li, K.-Q. Zhao, C. Redshaw, B. A.



Martínez Ortega, A. Y. Nuñez, T. A. Hanna in Patai's Chemistry of Functional Groups, Wiley 2014.

[2] (a) B. König and M.H. Fonseca, *Eur. J. Inorg. Chem.*, 2000, 2303–2310; (b) P. Lhoták, *Eur. J. Org. Chem.*, 2004, 1675–1692; (c) N. Morohashi, F. Narumi, N. Iki, T. Hattori, S. Miyano, *Chem. Rev.*, 2006, **106**, 5291–5316; (d) H. Tsue, K. Ishibashi, R. Tamura, *Top Heterocycl Chem.*, **2008**, *17*, 73–96; (e) K. Cottet, P. M. Marcos and P. J. Cragg, *Beilstein J. Org. Chem.*, 2012, **8**, 201–226; (f) R. Tamura, M. Miyata (eds.), *Advances in Organic Crystal Chemistry*, Chapter **13**, 2015, 241–261; (g) H. Takemura, T. Shinmyozu, H. Miura, I. U. Khan, *J. Incl. Phenom. Macro.*, 1994, **19**, 193–206.

[3] (a) C. Desroches, G. Pilet, S. A. Borshch, S. Parola, and D. Luneau, *Inorg. Chem.*, 2005, **44**, 9112–9120; (b) R. Kuriki, T. Kuwabara and Y. Ishii, *Dalton Trans.*, 2020, **49**, 12234–12241; (c) R. Kumar, Y. O. Lee, V. Bhalla, M. Kumar and J. S. Kim, *Chem. Soc. Rev.*, 2014, **43**, 4824–4870; (d) P. Thuéry, M. Nierlich, J. Vicens and H. Takemura, *Dalton Trans.*, 2000, 279–283; (e) C. Redshaw, M. Rowan, L. Warford, D. M. Homden, A. Arbaoui, M. R. J. Elsegood, S. H. Dale, T. Yamato, C. P. Casas, S. Matsui and S. Matsuura, *Chem. Eur. J.*, 2007, **13**, 1090–1107; (f) T. Xing, T. J. Prior, M. R. J. Elsegood, N. V. Semikolenova, I. E. Soshnikov, K. Bryliakov, K. Chen and C. Redshaw, *Catal. Sci. Technol.*, 2021, **11**, 624–636.

[4] M. Frediani, D. Sémeril, A. Marriotti, L. Rosi, P. Frediani, L. Rosi, D. Matt and L. Toupet, *Macromol. Rapid Comm.*, 2008, **29**, 1554–1560.

[5] (a) Z. Sun, Y. Zhao, O. Santoro, M. R. J. Elsegood, E. V. Bedwell, K. Zahra, A. Walton, and C. Redshaw, *Catal. Sci. Technol.*, 2020, **10**, 1619–1639; (b) O. Santoro, M. R. J. Elsegood, E. V. Bedwell, J. A. Pryce and C. Redshaw, *Dalton Trans.*, 2020, **49**, 11978–11996.

[6] A. W. Addison, T. N. Rao, J. Reedijk, J. van Rijn and G. C. Verschoor, *J. Chem. Soc., Dalton Trans.*, 1984, 1349–1356.

[7] (a) N. Li, J. –J. Liu, J. –W. Sun, B. –X. Dong, L. –Z. Dong, S. –J. Yao, Z. Xin, S. –L. Li and Y. Q. Lan, *Green Chem.*, 2020, **22**, 5325–5332; (b) X. –X. Yang, W. –D. Yu, X. –Y. Yi and C. Liu, *Inorg. Chem.*, 2020, **59**, 7512–7519; (c) X. –X. Yang, W. –D. Yu, X. –Y. Yi, L. –J. Li and C. Liu, *Chem Commun.*, 2020, **56**, 14035–14038.

[8] J. P. Fackler Jr., F. J. Kristine, A. M. Mazany, T. J. Moyer, and R. E. Shepherd *Inorg. Chem.*, 1985, **24**, 1857–1860.

[9] A. C. Cooper, J. C. Bollinger, J. C. Huffman and K. G. Caulton, *New J. Chem.*, 1998, **22**, 473–480.

[10] (a) C. Ludwig and M. R. Viant, *Phytochem. Anal.*, 2010, **21**, 22–32; (b) M. J. Walton, S. J. Lancaster and C. Redshaw, *ChemCatChem*, 2014, **6**, 1892–1898.

[11] (a) Z. Zhong, P. J. Dijkstra and J. Feijen, *J. Am. Chem. Soc.*, 2003, **125**, 11291–11298; (b) P. Hormnirun, E. L. Marshall, V. C. Gibson, A. J. P. White and D. J. Williams, *J. Am. Chem. Soc.*, 2004, **126**, 2688–2689.

[12] (a) F. Della Monica, E. Luciano, A. Buonerba, A. Grassi, S. Milione and C. Capacchione, *RSC Adv.*, 2014, **4**, 51262–51267; (b) P. Vanhoorne, P. Dubois, R. Jerome and P. Teyssie, *Macromolecules*, 1992, **25**, 37–44; (c) J. Kasperczyk and M. Bero, *Makromol. Chem.*, 1991, **192**, 1777–1787; (d) J. Kasperczyk and M. Bero, *Makromol. Chem.* 1993, **194**, 913–925; (e) N. Nomura, A. Akita, R. Ishii and M. Mizuno, *J. Am. Chem. Soc.*, 2010, **132**, 1750–1751; (f) G. Li, M. Lamberti, D. Pappalardo and C. Pellecchia, *Macromolecules*, 2012, **45**, 8614–8620.

[13] (a) B. Dhawan and C. D. Gutsche, *J. Org. Chem.*, 1983, **48**, 9, 1536–1539; (b) B. Masci, *J. Org. Chem.*, 2001, **66**, 1497–1499; (c) H. Takemura, A. Takahashi, H. Suga, M. Fukuda, and T. Iwanaga, *Eur. J. Org. Chem.*, 2011, 3171–3177.

[14] G. M. Sheldrick, *Acta Cryst.* 2015, **A71**, 3–8.

[15] G. M. Sheldrick, *Acta Cryst.* 2015, **C71**, 3–8.

[16] A. L. Spek, *Acta Cryst.* 2015, **C71**, 9–18.

